Glacial Lake Outburst Floods Simulation in the Yi'ong Zangbo River Basin Based on One-Dimensional Hydrodynamic Model

Qi Wang (wangqi@nwh.cn)
PowerChina: Northwest Engineering Corporation Limited

Hongyu Duan
Northwest Normal University

Na Liu
PowerChina: Northwest Engineering Corporation Limited

Zhishui Du
PowerChina: Northwest Engineering Corporation Limited

Pan Wang
PowerChina: Northwest Engineering Corporation Limited

Bo Yi
PowerChina: Northwest Engineering Corporation Limited

Jun Xu
PowerChina: Northwest Engineering Corporation Limited

Jian Huang
PowerChina: Northwest Engineering Corporation Limited

Research Article

Keywords: Glacial lake, GLOFs, Hydrodynamic modelling, the Jionglaco, Qinghai-Tibet Plateau

Posted Date: July 19th, 2021

DOI: https://doi.org/10.21203/rs.3.rs-709655/v1

Abstract

Glacial lake outburst floods (GLOFs) are a serious potential threat to the safety of life and property in downstream areas. In this study, moraine-dammed glacial lakes in the Yi'ong Zangbo River basin were recognized based on Landsat ETM+/TM/OLI images in 2000 and 2019. And the GLOFs for the Jionglaco, the largest glacial lake in this basin, was simulated using the one-dimensional hydrodynamic model. The results show that the total number and area of moraine-dammed glacial lakes in this basin increased by 10 (10.52%) and 5.49 km^2 (48.24%) from 2000 to 2019, in which the area of the Jionglaco increased by 3.22 km^2. The peak discharge at the breach outlet for five scenarios with different combinations of breach width (80 m and 120 m), depth (2.5 m and 5 m) and flood time (1.5 h and 3 h) are 489 m^3/s, 1327.43 m^3/s, 444.32 m^3/s, 617.47 m^3/s and 1570.61 m^3/s. With the addition of baseflow in river, the peak discharge at bridge site 15 138.93 km from Jionglaco are 1040.89 m^3/s, 1724.00 m^3/s, 1024.85 m^3/s, 1162.25 m^3/s and 1990.52 m^3/s. The combination of baseflow in river and the GLOFs discharge results in the increasing peak discharge in the further downstream region. However, the arrival of peak discharge in downstream areas is delayed, which increases the chances of people escaping. This study aims to provide some references for the prevention of GLOFs in this region.

1. Introduction

Glaciated regions are highly sensitive to climate change (Chevallier et al. 2011; Haeberli et al. 2013; Mool 2011; Wang and Zhou 2019; Shrestha and Aryal 2011; Xu et al. 2009) and recent global warming has led to an overwhelming retreat of glaciers and an increase in glacial meltwater, which results in the development of supraglacial lakes that coalesce to form proglacial lakes (Maskey et al. 2020). Some of glacial lakes are extremely dangerous because of the unstable geomorphology around them (Maskey et al. 2020). As the dams of these glacial lakes tend to be loose and unstable, the combination of external factors, such as the entry of ice avalanches and rock avalanches can lead to the collapse of dam and the release of water, forming glacial lake outburst floods (GLOFs). Consisting of a mixture of water and sediment, the GLOFs can travel at speeds more than tens of kilometers per hour for more than 100 km (Worni et al. 2014). Due to the high volume of emissions and long operational distances, lives and properties in downstream areas would generally suffer heavy losses (Maskey et al. 2020).

According to Zhang et al. (2015), there are a total of 5701 glacial lakes (> 0.003 km^2) in Qinghai-Tibet Plateau in 2015. Wang et al. (2020) synthetically identified 246 potential dangerous glacial lakes with a total area of 78.38 km^2 in the Qinghai-Tibet Plateau, in which glacial lakes with very high and high integrated risk of GLOFs disasters are concentrated on the central Himalayas, the central-eastern Nyainqentanglha range, and the southern Tanggula mountains. Both the Jionglaco and the Jiongpuco were included in these potential dangerous glacial lakes. The Jionglaco is a large glacial lake in the eastern part of the Nyainqentanglha range, located in the Yi'ong Zangbo River basin, where three historical GLOFs have occurred, which all caused significant damage to the downstream area (Yao et al. 2014; Sun et al. 2014; Liu et al. 2021). The Jionglaco is larger than all three glacial lakes that have been breached and has a rapid area expansion in recent years. The Jiongpuco is a moraine-dammed glacial lake in the southwest of the Jionglaco with area expansion in the past two decades. Moreover, there are many settlements, roads and bridges in the downstream area, so the GLOFs simulation for the Jionglaco is urgent, which can provide data support and theoretical basis for GLOFs prevention and mitigation in this region.

2. Study Area

Yi'ong Zangbo River basin (30°05'–31°03' N, 92°52'–95°19' E), situated in the southern aspect of the Nyainqêntanglha range, is fed by Yi'ong Zangbo River and covers an area of 13,533 km^2 (Fig. 1(a)). The terrain is high in the west and low in the east, with an average altitude of over 4,000 m (Fig. 1(b)). The average annual precipitation is 958 mm, and the peak precipitation occurs in the Indian monsoon season from May to September, which accounts for 74.9% of the annual total precipitation according to records from the nearest meteorological station in Bomi. The mean annual temperature is 8.8 ℃, with average temperatures of 16.7 ℃ in July and 0.28℃ in January (Ke et al. 2013, 2014). The massive topographic landforms together with the Indian monsoons leads to the development of distinct temperate valley glaciers and a substantial number of glacial lakes (Fig. 1(c)). The Jionglaco (30˚39'44" N, 94˚29'01" E), located in the Jinling Township, Bianba County, which is a typical moraine-dammed glacial lake fed by the huge maritime glacier (Fig. 1(c)). The glacier melted dramatically, and the glacial lake expanded rapidly towards the glacier terminus with the area of 5.68 km^2 in 2020. Meanwhile, there are many villages and bridges located in the downstream area of the glacial lake (Fig. 1(c)).

3. Materials And Methods

3.1 Glacier and glacial lake mapping

As the primary source of medium spatial resolution Earth observations, the Landsat series images is an important data source for studying glacier and glacial lake changes (Wood et al. 2008; Chander et al. 2009). In this study, a total of six scenes of Landsat TM/ETM+/OLI images with little snow and cloud cover downloaded from the United States Geological Survey (USGS) (http://glovis.usgs.gov/) were used to delineate the outlines of glacial lakes in 2000 and 2019 (Table 1). The spatial resolution of Landsat TM is 30 m. However, Landsat ETM+/OLI images are available in multi-spectral band 30 m and panchromatic band 15 m, fusing the two data results in multi-spectral data with spatial resolution of 15 m, which is beneficial for accurate extraction of the glacial lake outlines. And one scene of GaoFen-6 image downloaded from the Chinese High resolution Earth Observation System (CHEOS) (https://login.cheosgrid.org.cn/) was used to delineate the outlines for the Jionglaco and the mother glacier in 2020, the downstream river channel and the sections from left bank to right bank. The spatial resolution of the multi-spectral band and panchromatic band for GF-6 images are 4 m and 2 m, respectively. After the same processing as Landsat ETM+/OLI, the multi-spectral image with a spatial resolution of 2 m was obtained, which clearly shows the outlines of the Jionglaco, the mother glacier and the river channel. Because GF-6 image does not match well with Landsat image, it was orthorectified using ALOS PALSAR DEM data with a spatial resolution of 12.5 m.

Glacial lakes are generally small in area and scattered in the overall region, making them easily confused with the surrounding mountain shadows and snow and other feature information when automated extraction is undertaken. Ultimately, a lot of manual checking and revision work after automated extraction is essential (Yang et al. 2019). In contrast, manual visual interpretation can flexibly adapt to the vectorization of glacial lakes of complex background information and large differences in image quality. Meanwhile, the expert empirical knowledge is good at controlling the impact of adverse factors such as shadow, snow, and cloud cover on glacial lake extraction (Yang et al. 2019). Therefore, in this study, manual visual interpretation method was used for extraction of glacial lake outlines, and the area error was controlled within one mixed pixel.

Table 1
Remote sensing images used in this study

Path/Row	Date	Sensors	Resolution/m	Source
136/039	1999-09-22	Landsat TM	30	The United States Geological Survey (http://glovis.usgs.gov/)
136/039	2000-05-11	Landsat ETM+	15/30	
135/039	2000-05-04	Landsat ETM+	15/30	
135/039	2019-06-02	Landsat OLI	15/30	
136/039	2019-08-28	Landsat OLI	15/30	
136/039	2019-11-16	Landsat OLI	15/30	
—	2020-08-06	GF-6 PMS	2/4	The Chinese High resolution Earth Observation System (https://login.cheosgrid.org.cn/)

3.2 MIKE11 model construction

MIKE11 is a specialized software developed by the Danish Hydraulic Institute (DHI) for one-dimensional hydrodynamics, flood forecasting and dam failure (MIKE11 User Manual 2003). Jain et al. (2012) did the GLOFs simulation using one-dimensional MIKE11 model for the largest glacial lake of a river basin in the Garwhal Himalaya, India. Thakur et al. (2016) carried out the GLOFs simulation for the six hydroelectric power projects in Dhauliganga river of Alaknanda Basin based on the MIKE11 model. Riyaz et al. (2018) used the MIKE11 model to generate the peak hydrographs at the lake and other vulnerable sites downstream. The above studies demonstrate that the Hydrodynamics and Dam Breach modules of MIKE11 model have powerful capabilities for the numerical simulation of rivers and the replication and calculation of dam breaching processes. Therefore, the MIKE11 model was used for the simulation of GLOFs in this study. The Hydrodynamics module (HD) and Dam Failure module of MIKE11 contains an implicit, finite difference computation of unsteady flows in river and has powerful functions for numerical river simulation and dam failure process calculation (Jain et al. 2012). The model is built with six files: simulation file, river network file, section file, boundary file, parameter file, time series file and result file (Table 2).

Table 2
Description of MIKE11HD modeling files

File name	Filename suffix	Data and function	Data source
Simulation file	.sim11	Integrating other files, start and end time of the simulation, simulation time step	—
Parameter file	.hd11	Initial conditions: water level, discharge, bed resistance	Measured data, reference data
Result file	.res11	Calculation results and post-processing	—
Time series file	.dfs0	Time-varying discharge, water level and dam structure	Measured data, hypothetical data
River network file	.nwk11	River path, length and network	GF-6 PMS
Cross-section file	.xns11	Location and shape of cross-section	GF-6 PMS, ALOS DEM, SRTM DEM
Boundary file	.bnd11	Discharge, discharge-level curve, dam structure, tributary inflow	Measured data, hypothetical data

3.2.1 River network, cross-sections, and boundary condition

River network is used to define the modeling flood path, which was represented by the manually extracted river centerline from GF-6 PMS images (Fig. 2(a)). Cross-sections are used to reflect the topography of the river channel, which determine the state and calculation of the flood evolution process (Fig. 2(b)). The thalweg reflects longitudinal specific drop of the simulated river channel, which impacts the travel speed and potential energy of the flood (Fig. 2(c)).

Cross-section is the data that has the greatest impact on the model and can usually be obtained from actual measurements and DEM data. The former is more accurate but time consuming and labor intensive. By contrast, the latter is easy to obtain but the accuracy is influenced by the accuracy of the adopted DEM data. Both measured cross-sections (in Yi'ong Zangbo River) and DEM-based cross-sections (by ALOS PULSAR Digital Elevation Model (DEM) (12.5 m)) (in Xiaqu River) are included in this study. The DEM-based cross-sections are extracted roughly every 500 ~ 1000 m along the Xiaqu River (Fig. 1(b)(c)).

Boundary file defines the interaction between the model and the external environment, which is divided into two types open boundary and additional boundary (MIKE11 User Manual 2003). In this study, upstream open boundary of the

model is the glacial meltwater entering the glacial lake, because the discharge is relatively small and has slight influence on the model, a steady flow 1 m^3/s was taken. The downstream open boundary is the field measured water level-discharge relationship at the bridge location downstream of the Bazhui village (Fig. 1(c), Fig. 2(d)). In addition, five lateral entry flows were set as internal boundary in this model representing the baseflow of the river channel consisting of the confluent tributaries which is 637.5 m^3/s during flood season (May to October) according to the monitoring data.

3.2.2 LULC and Manning's N

Friction of the river channel to a given flow is determined by the Manning's roughness coefficient (Coon 1998), which is dependent on the land use and land cover (LULC) of the modeling river channel in the study area. In the study, the value of Manning's N of cross-sections were obtained from the GLC10 LULC product (http://data.ess.tsinghua.edu.cn/fromglc10_2017v01.html) with the spatial resolution of 10 m. The extent to which all transect widths covered along the river channel was extracted for the analysis of LULC types in this region. A total of nine types were identified in the potential flood area, of which forest holds the highest proportion of 51.43%, followed by grassland of 21.6% and bareland of 17%, the Manning's N values for them are 0.035, 0.034 and 0.04, respectively. Westoby et al. (2015) stated the value of 0.05 as a global Manning's N for a flood plain setting consisting of pebbles, cobbles, and boulders. In this study, we took a weighted average of the Manning's N value for the different LULC types based on their area percentages, and finally the value of 0.035 was chose as the global Manning's N value for the given flow area.

3.2.3 Volume and depth of glacial lake

Lake bathymetric data is one of the most crucial parameters in the dynamic modeling of GLOFs (Westoby et al. 2014). However, glacial lakes are usually distributed in relatively inaccessible environments, making field studies be complicated. Hindered by turbidity, the derivation of reflectance-depth relationships of a lake from satellite sensor has not yet been reliably achieved (Box and Ski 2007). Consequently, the most of studies adopted an empirical approach to calculate the volume or depth of a glacial lake (Evans 1986; O'Connor et al. 2001; Huggel et al. 2002; Yao et al. 2012; Loriaux and Cassassa 2013; Carrivick and Quincey 2014). In this study, the most widely used relationships proposed by Huggel et al. (2002) was used to estimate the water storage and depth of the Jionglaco.

$$D = 0.104A^{0.42} \quad (1)$$

$$V = 0.104A^{1.42} \quad (2)$$

where V is volume (m^3) and D is mean depth of a glacial lake (m); A is the surface area of a glacial lake (m^2).

3.2.4 GLOFs modeling

Triggers such as ice/snow avalanches, rock fall or calving processes usually generate impulse waves capable of initiating an overtopping failure ultimately leading to a GLOF event (Ashim et al. 2019). In addition, extreme weather conditions with heavy precipitation or sudden warming can cause the water level of glacial lake to rapidly rise and even overflow. Based on the high-resolution imagery and 3D terrain rendering scene view of ArcGIS Earth software, the mean water level of the Jionglaco was measured as 3915.5 m, the width of the dam as about 394 m. The moraine dam is flat, there is a water outlet of about 40 m width on the right side. The dam rises slowly from the outlet to the both ends, reaching a maximum height of approximately 3920.5 m. Assuming that the breach depth of dam is half (2.5 m) and full (5 m) of the elevation difference between the highest point of the dam and both the lake surface and the outlet river, the breach width of dam is twice (80 m) and triple (120 m) the width of the outlet, and the time of the

peak flood is 1.5 h and 3 h respectively, thus five breach scenarios were designed to simulate the flood process (Table 3).

Table 3
Model parameters for different GLOFs scenarios

Parameters	Scenario 1	Scenario 2	Scenario 3	Scenario 4	Scenario 5
Time of breach (h)	1.5	1.5	3	3	3
Breach width (m)	80	80	80	120	120
Breach depth (m)	2.5	5	2.5	2.5	5
Discharge volume (×106 m3)	15.70	30.98	15.70	15.70	30.98
Percentage of released water volume (%)	3.86	7.61	3.86	3.86	7.61

4. Results

4.1 Status and changes of glacial lake

There were 95 moraine-dammed glacial lakes with a total area of 11.38 km^2 in the Yi'ong Zangbo River basin in 2000 and 105 moraine-dammed glacial lakes with a total area of 16.87 km^2 in the basin in 2019, with increasing ratio in number and area of 10.52% and 48.24% (Table 4). In 2000, there were three glacial lakes with area larger than 1.00 km^2, corresponding to the total area of 4.58 km^2. In 2019, the number of glacial lakes of larger than 1.00 km^2 remained three, however the total area has increased to 8.38 km^2 with the ratio of 82.97%. The number and total area of glacial lakes in area intervals of 0.10 ~ 1.00 km^2 and 0.01 ~ 0.10 km^2 were both increased. However, the number and total area of glacial lakes smaller than 0.01 km^2 both decreased during the past decade, which does not indicate that the growth of glacial lakes has stagnated or regressed, but rather that the smaller lakes have been subsumed into other larger size intervals due to their expansion. As the largest moraine-dammed glacial lake, the Jionglaco's area has increased from 2.47 km^2 in 2000 to 5.69 km^2 in 2020 with the average rate of 0.16 km^2/a.

There were three historical GLOFs in Yi'ong Zangbo River basin, they are Coga (GLOF date: 20090729) (Yao et al. 2014), Ranzeriaco (GLOF date: 20130705) (Sun et al. 2014), and Jiwuco (GLOF date: 20200626) (Liu et al. 2021). The areas of the above three lakes before and after the outburst were 0.42 km^2, 0.58 km^2 and 0.58 km^2 as well as 0.29 km^2, 0.25 km^2 and 0.27 km^2, respectively. At present, the areas for three glacial lakes are 0.36 km^2, 0.28 km^2 and 0.27 km^2. The area of the Coga increase rapidly (24.14%), reaching 85.71% of the area before the GLOF event. In contrast, the Ranzeriaco has a little increase (12%). Jiwuco has a stable area due to the relatively recent time of the GLOF event.

Table 4
Number and area of moraine-dammed glacial lakes in 2000 and 2019

Year/change ratio	≥ 1.00 km^2		0.1 ~ 1.00 km^2		0.01 ~ 0.10 km^2		< 0.01 km^2		Total	
	Number	Area	Number	Area	Number	Area	Number	Area	Number	Area
2000	3	4.58	19	4.45	59	2.22	14	0.12	95	11.38
2019	3	8.38	23	6.02	71	2.40	8	0.07	105	16.87
Change ration (%)	0	+ 82.97	+ 21.05	35.28	+ 20.34	+ 8.11	-42.86	-41.67	+ 10.52	+ 48.24

4.2 GLOFs simulation

A lot of bridges and villages are distributed in the downstream valley of the Jionglaco. Based on Google Earth imagery and ArcGIS Earth imagery, a total of 15 bridge sites and 20 villages were identified in the study river channel. We only make statistic for GLOFs hydrological processes at the 15 bridge sites, including peak flow, flooding of breach, water level and flood propagation time. Depending on the height of the dam and the width of the outlet of the Jionglaco, five different scenarios with different combinations of breach width (80 m and 120 m), depth (2.5 m and 5 m) and flood peak time (1.5 h and 3 h) were simulated (Table 3). Each scenario produces the different magnitude of flood peak at breach outlet (Fig. 3). The results show that scenario 5 produces the maximum GLOF peak discharge of 1570.61 m^3/s at the conditions of flood peak time of 3 h, breach width and depth of 120 m and 5 m. Scenario 2 produces the second maximum GLOF peak discharge of 1327.43 m^3/s, it has the same breach depth of 5 m however the flood peak time and breach width are 1.5 h and 80 m, respectively. Scenario 3 produces the minimum GLOF peak discharge of 444.32 m^3/s with condition of the flood peak time of 3 h, breach width and depth of 80 m and 2.5 m, respectively.

The GLOFs peak discharge, flood propagation time, water depth and flow hydrograph at the downstream bridge sites were generated for five scenarios (Table 5 and Fig. 4). Considering only the peak discharge caused by GLOFs, it decreases the further away from the lake due to surface frictional resistance and head loss along river path. From breach outlet to bridge site 15, the peak discharge of five scenarios were decreased from 489.00 m^3/s, 1327.43 m^3/s, 444.32 m^3/s, 617.47 m^3/s, 1570.61 m^3/s to 403.39 m^3/s, 1086.5 m^3/s, 387.35 m^3/s, 524.75 m^3/s, 1353.02 m^3/s, with the reduction ratios of 17.50%, 18.15%, 12.82%,15.02% and 13.85% (Table 5). However, different bridge sites from upstream to downstream show different change trends due to the dual effects of lateral runoff and flooding. Form bridge site 1 to bridge site 4, the peak discharge of five scenarios were reduced from 473.37 m^3/s, 1285.58 m^3/s, 433.78 m^3/s, 600.72 m^3/s and 1532.71 m^3/s to 455.17 m^3/s, 1227.7 m^3/s, 421.72 m^3/s, 580.25 m^3/s and 1479.28 m^3/s respectively (Table 5 and Fig. 4). However, because of a lateral runoff between bridge site 4 and bridge site 5, the peak discharge at the bridge site 5 of five scenarios were respectively increased to 521.35 m^3/s, 1272.44 m^3/s, 491.72 m^3/s, 644.69 m^3/s, 1523.35 m^3/s. From bridge site 5 to bridge site 9, the peak discharge gradually decreased from upstream to downstream and they were 512.68 m^3/s, 1228.08 m^3/s, 488.44 m^3/s, 632.22 m^3/s, 1470.96 m^3/s at bridge site 9 for five scenarios (Table 5 and Fig. 4). From bridge site 9 to bridge site 15, the peak discharge flow increases continuously due to the addition of lateral runoff, with peak discharges of 1040.89 m^3/s, 1724.00 m^3/s, 1024.85 m^3/s, 1162.25 m^3/s and 1990.25 m^3/s for five scenarios, respectively (Table 5 and Fig. 4).

Bridge sites 3, 5, 9, 11, 14 and 15 are the locations with a high density of settlements (Fig. 1(c)). In the scenario with the maximum peak discharge (1570.61 m^3/s) at the breach outlet, the peak discharges at above bridge sites are 1505.31 m^3/s, 1523.35 m^3/s, 1470.96 m^3/s, 1874.61 m^3/s, 1924.24 m^3/s and 1990.52 m^3/s, respectively (Table 5). The peak discharge decreases between bridge site 5 and bridge site 9, after which all show an increasing trend. The flood propagation times for above bridge sites are 23 minutes, 1 hour and 8 minutes, 2 hour and 8 minutes, 3 hour and 20 minutes, 4 hour and 11 minutes, 5 hour and 23 minutes, respectively (Table 5). Although the peak discharge in the upstream area is smaller than the downstream area, flood propagation time is short, leaving insufficient time for people's transfer. However, the longer flood propagation time in downstream areas provides sufficient time for people to move to safe areas if timely warnings are received from upstream areas.

The modelled water depth is prone to uncertainty due to variations in datum between observed water level measured from mean sea level and modelled water level based on WGS-84 datum (Thakur et al. 2016). The DEM data used to extract the cross-sections also affect the accuracy of the water depth, and if the DEM data is of high accuracy, the error will be relatively small. The deepest water depth is at bridge site 15 and the shallowest is at bridge site 3, which is

influence both by the shape of cross-section and the depth of baseflow. Deeper and narrower cross-section as well as more discharge can lead to deeper water depths. In this study, the 6.73 m increase of water level at bridge 15 in the extreme scenario (Table 5), whereas at bridge 3 the rise is only 2.55 m.

5. Discussion

5.1 Potential GLOFs of the Jionglaco

The glacial lakes with high risk of breaching usually has the following characteristics: (1) being terminal moraine-dammed glacial lakes (Cui et al. 2003 and Chen et al. 2004) with the loose material and ice cores comprised as well as unstable and steep structured dam (Xu and Feng 1989); (2) having the relatively large area, area change and complete lake basin topography (Richardson and Reynolds 2000); (3) being close to or directly connected to the termini of its mother glacier which has steep slopes in the tongue section and fast change rate (Chen et al. 2003, 2008, 2009); (4) having the small crest. The Jionglaco is a typical terminal moraine-dammed glacial lake with a huge area of 5.69 km^2 in 2020, which is close to the maximum size of glacial lake in the Qinghai-Tibet Plateau in 2015 (Yang et al. 2019). The Jionglaco is directly connect to its mother glacier, which has retreat rapidly in company with the lake expansion. It has an intact lake basin topography and the average height difference between water level and dam is only 5 m. Therefore, the Jionglaco was identified as a potentially hazardous glacial lake by Duan et al. (2020) and Wang et al. (2020). However, the dam of the Jionglaco is very flat and a natural outlet of 40 m in width has formed, which is a favorable condition for maintaining the water balance of the glacial lake and reduces the impact of hydrostatic pressure on the dam. In addition, the dam has been reinforced by the local government to prevent a breach disaster. The presence or absence of ice cores within the moraine dams cannot be determined at present and further fieldwork is required. The slope in the mother glacier snout is smaller than 10°, which lowers the possibility of ice avalanche into the lake.

The main direct causes of GLOFs on the Qinghai-Tibet Plateau includes that (1) ice body, glacier tongue and mountain boulders collapse into lake, causing surges that overflow the dam and lead to dam failure (Clague and Evans 2000); (2) a sudden large increase in glacial meltwater or a sudden precipitation event that causes the lake level to rise and overtop the dam, leading to the dam to break (Richardson and Reynolds 2000); (4) melting ice cores in the dam body, infiltration water erosion, leading to the expansion of the pipe surge and eventually the failure of the dam (Yang et al. 2019). The main causes of GLOFs in the south-eastern Qinghai-Tibet Plateau are ice avalanches and ice slides, followed by pipe surges (Pu 2004). In contrast, GLOFs in the Himalayas are mainly caused by ice avalanches and ice slides (Richardson and Reynolds 2000). For the Jionglaco, the possibility of ice avalanche and rockfall caused GLOFs is relatively low due to the gentle-sloped glacier tongue. Second, because the area of the glacial lake is very large, the larger the area has the stronger bearing capacity for the mass entering the lake. Therefore, the Jionglaco is more resistant to disturbances caused by substances entering it, reducing the pressure on the dam from water fluctuations (Wang et al. 2016). However, the occurrence of GLOFs cannot be ruled out in extreme cases due to the injection of large volumes of water, which may be caused by the large increased meltwater from mother glacier due to abnormally high temperatures, extensive basin inflow due to extreme precipitation and inflow from other GLOFs. A high-risk glacial lake, Jiongpuco is located to the southwest of the Jionglaco, which has also undergone an area expansion in the past 20 years (Duan et al. 2020; Wang et al. 2020). Jiongpuco's outflow directly injects into the Jionglaco, therefore the hypothetical GLOF of Jiongpuco will probably produce a large disturbance to the Jionglaco, thus triggering the occurrence of GLOF in the Jionglaco. In addition, there are a lot of floating ice on the lake in the summer of some years, which may collect at the estuary, and then block the lake outlet and rise the water level of glacial lake, and eventually cause the overflow of lake.

5.2 Limitation

The water level-surface area relationship is a critical input parameter of the simulation, which is the data representation of the breaching glacial lake and was calculated by empirical formula in this study. The empirical formula used to calculate the depth and volume of a glacial lake is a regression function of its area. Due to the huge surface area, the depth and volume of the Jionglaco are likely to be overestimated. However, the use of empirical formulas to calculate volume and depth is the only means when actual measurement data is lacking. In the future, the measured lake depth data will help to improve the accuracy of the simulation.

Currently, there is a lack of adequate grasp of the mechanism of glacial lake outburst flood and the formation of the breaching outlet. The simulation of GLOFs is an approximate physical phenomenon and carried out according to certain parameters, such as the width, depth of the outlet and duration of the breach discharge reaching the maximum value. Therefore, these parameters determine the magnitude of the peak discharge of the breach. In this study, the width of the breach is assumed twice and three times the current flow outlet, the depth of the breach is assumed half and full of the current average height of the dam and the outburst duration is assumed 1.5 h and 3 h referencing to an already GLOF event of 2.5 h in this basin.

In addition, the evolution of flood in the downstream area is influenced by the shape of the cross-sections, which are the reflection of the downstream river topography. The accuracy of the cross-sections is determined by the accuracy of field measurements or the accuracy of the DEM data. High-quality cross-section data is a guarantee of high-quality simulations. The measured cross-section data has a high degree of accuracy, but the DEM-based data can only reflect the topography above the water surface.

Despite the difficulty in accessibility of data, we simulated five GLOFs scenarios based on different breach width, depth and flood peak time using a one-dimensional model. Meanwhile, the flood characteristics at the breach outlet and the 15 bridge sites in the downstream area were analyzed. Generally, the study can provide some reference for the subsequent prevention, mitigation, and control of flood in the region.

6. Conclusion

The increase of number and area of glacial lakes caused by the glaciers retreat in context of global warming also increases the likelihood of GLOFs which pose a huge threat to lives and property in downstream areas. We delineated 95 moraine-dammed glacial lakes with a total area of 11.38 km^2 in 2000 and 105 moraine-dammed glacial lakes with a total area of 16.87 km^2 in 2019 in the Yi'ong Zangbo River basin. The largest glacial lake in the basin, the Jionglaco, has experienced a dramatic expansion over the past 20 years with an area increase of 3.22 km^2. When the breach width, depth and flood peak time is set as 120 m, 5 m and 3 h, the peak discharge of 1570.61 m^3/s at the breach outlet is the largest. And the smallest peak discharge at breach outlet occurs at the breach width of 80 m, breach depth of 2.5 m and the flood peak time of 3 hours.

In the scenario of the largest peak discharge (1570.61 m^3/s) at the breach outlet, the peak discharges at bridge sites 3, 5, 9, 11, 14 and 15 where the downstream settlements are densely distributed are 1505.31 m^3/s, 1523.35 m^3/s, 1470.96 m^3/s, 1874.61 m^3/s, 1924.24 m^3/s and 1990.52 m^3/s with the flood propagation times of 23 minutes, 1 hour and 8 minutes, 2 hour and 8 minutes, 3 hour and 20 minutes, 4 hour and 11 minutes, 5 hour and 23 minutes, respectively. Compared with downstream areas, the upstream area is at higher risk due to the shorter flood propagation time. If there is early warning communication, the loss of life and property of people in the downstream area will be greatly reduced. Although based on scenario simulations with assumed parameters, this study provides a meaningful reference for understanding and GLOFs in the region.

Declarations

Compliance with ethical standard:

Conflicts of interest: The authors have no conflicts of interest to declare that are relevant to the content of this article.

References

1. Ashim S, Ajanta G, Anil VK (2019) Hydrodynamic moraine-breach modeling and outburst flood routing-A hazard assessment of the South Lhonak lake, Sikkim-ScienceDirect. Science of The Total Environment 668:362–378
2. Box JE, Ski K (2007) Remote sounding of Greenland supraglacial melt lakes: implications for subglacial hydraulics. J Glaciol 53(181):257–265
3. Carrivick JL, Quincey DJ (2014) Progressive increase in number and volume of ice-marginal lakes on the western margin of the Greenland Ice Sheet. Global Planet Change 116:156–163
4. Coon WF (1998) Estimation of roughness coefficients for natural stream channels with vegetated banks. US Geological Survey Water Supply Paper, p 2441
5. Chevallier P, Pouyaud B, Suarez W, Condom T (2011) Climate change threats to environment in the tropical Andes: glaciers and water resources. Reg Environ Change 11(1):179–187
6. Chander G, Markham BL, Helder DL (2009) Summary of current radiometric calibration coefficients for Landsat MSS, TM, ETM, and EO-1 ALI sensors. Remote sensing of Environment 113(5):893–903
7. Cui P, Ma DT, Chen NC (2008) The initiation, motion and mitigation of debris flow caused by a glacial lake outburst flood, western Norway. Landslides 5(3):271–280
8. Chen XQ, Chen NS, Cui P (2004) Calculation of discharge of debris flow induced by glacier lake outburst. Journal of Glaciology Geocryology 26(3):207–214
9. Cheng ZL, Tian JC, Zhang ZB (2009) Debris flow induced by glacial lake break in southeast Tibet. Earth Sci Front 16(6):207–214
10. Cheng ZL, Zhu PY, Dang C, Liu JJ (2008) Hazards of debris flow due to glacier lake outburst in southeastern Tibet. Journal of Glaciology Geocryology 30(6):954–959
11. Cheng ZL, Zhu PY, Dang C, Gong YW (2003) Typical debris flow triggered by ice-lake break. J Mt Sci 21(6):716–720
12. Clague JJ, Evans SG (2000) A review of catastrophic drainage of moraine-dammed lakes in British Columbia. Quatern Sci Rev 19(17–18):1763–1783
13. Duan HY, Yao XJ, Zhang DH, Qi MM, Liu J (2020) Glacial Lake Changes and Identification of Potentially Dangerous Glacial Lakes in the Yi'ong Zangbo River Basin. Water 12(2):538
14. Evans SG (1986) Landslide Damming in the Cordillera of Western Canada. Landslide Dams: Processes, Risk and Mitigation 3:111–130
15. Huggel C, Kb A, Haeberli W, Teysseire P, Paul F (2002) Remote Sensing based assessment of hazards from glacier lake outbursts: a case study in the Swiss alps. Can Geotech J 39(2):316–330
16. Haeberle W, Huggel C, Paul F, Zemp M (2013) Glacial responses to climate change. In: Shroder JF (ed) Treatise on geomorphology. Academic Press, San Diego, pp 152–175
17. Jain SK, Lohani AK, Singh RD, Chaudhary A, Thakural LN (2012) Glacial lakes and glacial lake outburst flood in a Himalayan basin using remote sensing and GIS. Nat Hazards 62(3):887–899

18. Ke CQ, Kou C, Ludwig R, Qin X (2013) Glacier velocity measurements in the eastern Yigong Zangbo basin, Tibet, China. J Glaciol 59(218):1060–1069
19. Ke CQ, Han YF, Kou C (2014) Glacier Change in the Yigong Zangbu Basin, Tibet, China (1988 to 2010). Dragon 3 Mid Term Results
20. Loriaux T, Casassa G (2013) Evolution of glacial lakes from the Northern Patagonia Icefield and terrestrial water storage in a sea-level rise context. Global Planet Change 102:33–40
21. Liu JK, Zhou LX, Zhang JJ, Zhao WY (2021) Characteristics of Jiwengcuo GLOF, Lhari county, Tibet. Geological Review 67:Supply1
22. Mool PK, Maskey PR, Koirala A, Joshi SP, Wu L, Shrestha AB (2015) Glacial lakes and glacial lake outburst floods in Nepal. ICIMOD, Kathmandu
23. Maskey S, Kayastha RB, Kayastha R (2020) Glacial lakes outburst floods (GLOFs) modelling of Thulagi and lower Barun glacial lakes of Nepalese Himalaya. Progress in Disaster Science 7:100106
24. MIKE11 User Manual (2003) https://www.tu-braunschweig.de/Medien-DB/geooekologie/mike-11-short-introduction-tutorial
25. O'Connor JE, Iii J, Costa JE (2001) Debris flows from failures of neoglacial-age moraine dams in the three sisters and mount Jefferson wilderness areas, Oregon. Econ Theor 4(1606):11–40
26. Pu JC, Yao TD, Wang NL, Su Z, Shen YP (2004) Fluctuations of the glaciers on the Qinghai-Tibetan Plateau during the past century. Journal of Glaciology Geocryology 26(5):517–522
27. Richardson SD, Reynolds JM (2000) An overview of glacial hazards in the Himalayas. Quatern Int 65(99):31–47
28. Sun MP, Liu SY, Yao XJ, Li L (2014) The cause and potential hazard of glacial lake outburst flood occurred on July 5, 2013 in Jiali County, Tibet. Journal of Glaciology Geocryology 36(1):158–165
29. Shrestha AB, Aryal R (2011) Climate change in Nepal and its impact on Himalayan glaciers. Reg Environ Change 11(1):65–77
30. Thakur PK, Aggarwal S, Aggarwal SP, Jain SK (2016) One-dimensional hydrodynamic modeling of GLOF and impact on hydropower projects in Dhauliganga river using remote sensing and GIS applications. Nat Hazards 83(2):1057–1075
31. Wang SJ, Zhou LY (2019) Integrated impacts of climate change on glacier tourism. Advances in Climate Change Research 10(2):71–79
32. Wang SJ, Che YJ, Ma XG (2020) Integrated risk assessment of glacier lake outburst flood (GLOF) disaster over the Qinghai–Tibetan Plateau (QTP). Landslides 6410
33. Woodcock CE, Allen R, Anderson M, Belward A, Bindschadler R, Cohen W, Gao F, Goward SN, Helder D, Helmer E, Nemani R (2008) Free access to Landsat imagery. Science 320(5879):1011
34. Wang X, Liu SY, Ding YJ (2016) Evaluation methods and applications of moraine lake outburst hazards in the Chinese Himalayas. Science Press, Beijing
35. Worni R, Huggel C, Clague JJ, Schaub Y, Stoffel M (2014) Coupling glacial lake impact, dam breach, and flood processes: a modeling perspective. Geomorphology 224:161–176
36. Westoby MJ, Glasser NF, Brasington J, Hambrey MJ, Quincey DJ, Reynolds JM (2014) Modelling outburst floods from moraine-dammed glacial lakes. Earth-Sci Rev 134:137–159
37. Westoby M, Brasington J, Glasser N, Hambrey M, Reynolds J, Hassan M, Lowe A (2015) Numerical modelling of glacial lake outburst floods using physically based dam-breach models. Earth Surf Dyn 3(1):171–199

38. Xu JC, Grumbine RE, Shrestha A, Eriksson M, Yang X, Wang Y, WILKES A (2009) The melting Himalayas: cascading effects of climate change on water, biodiversity, and livelihoods. Conserv Biol 23(3):520–530
39. Xu DM, Feng QH (1989) Dangerous glacial lake and outburst features in Xizang Himalayas. Acta Geogr Sin 44(3):343–352
40. Yang CD, Wang X, Wei JF, Liu Q, Lu AX, Zhang Y, Tang Z (2019) Chinese glacial lake inventory based on 3S technology method. Acta Geogr Sin 74(3):544–556
41. Yang RM, Zhang TJ, Zhu LP, Ju JT (2019) Laigu glacial lake variation and its outburst flood risk in southeast Tibetan Plateau. Quaternary Sciences 39(5):1171–1180
42. Yao XJ, Liu SY, Sun MP, Wei J, Guo WQ (2012) Volume calculation and analysis of the changes in moraine-dammed lakes in the north Himalaya: a case study of Longbasaba lake. J Glaciol 58:753–760
43. Yao XJ, Liu SY, Sun MP, Zhang XJ (2014) Study on the Glacial Lake Outburst Flood Events in Tibet since the 20th Century. Journal of Natural Resources 8:1377–1390
44. Zhang GQ, Yao TD, Xie HJ, Wang WC (2015) An inventory of glacial lakes in the Third Pole region and their changes in response to global warming. Global Planet Change 131:148–157

Table 5

Due to technical limitations, Table 5 is only available as a download in the Supplemental Files section.

Figures

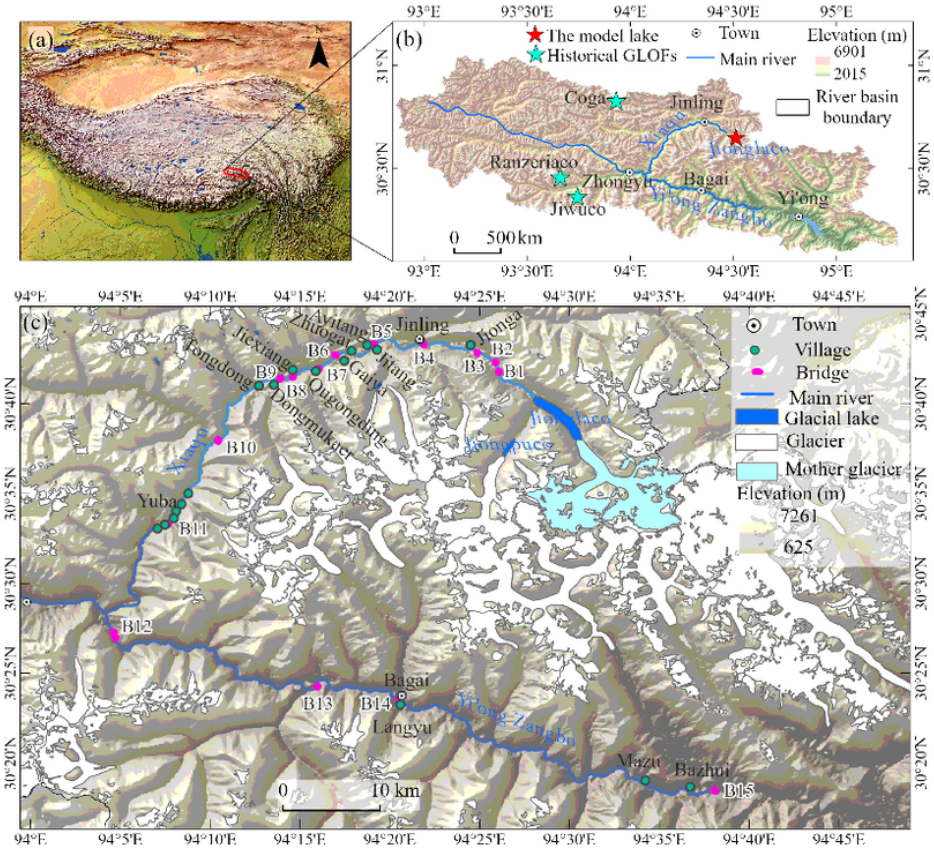

Figure 1

The study area showing that (a) location of Yi'ong Zangbo River basin in Qinghai-Tibet Plateau; (b) historical GLOFs and Jionglaco; (c) towns, villages, and bridges along the downstream river of Jionglaco.

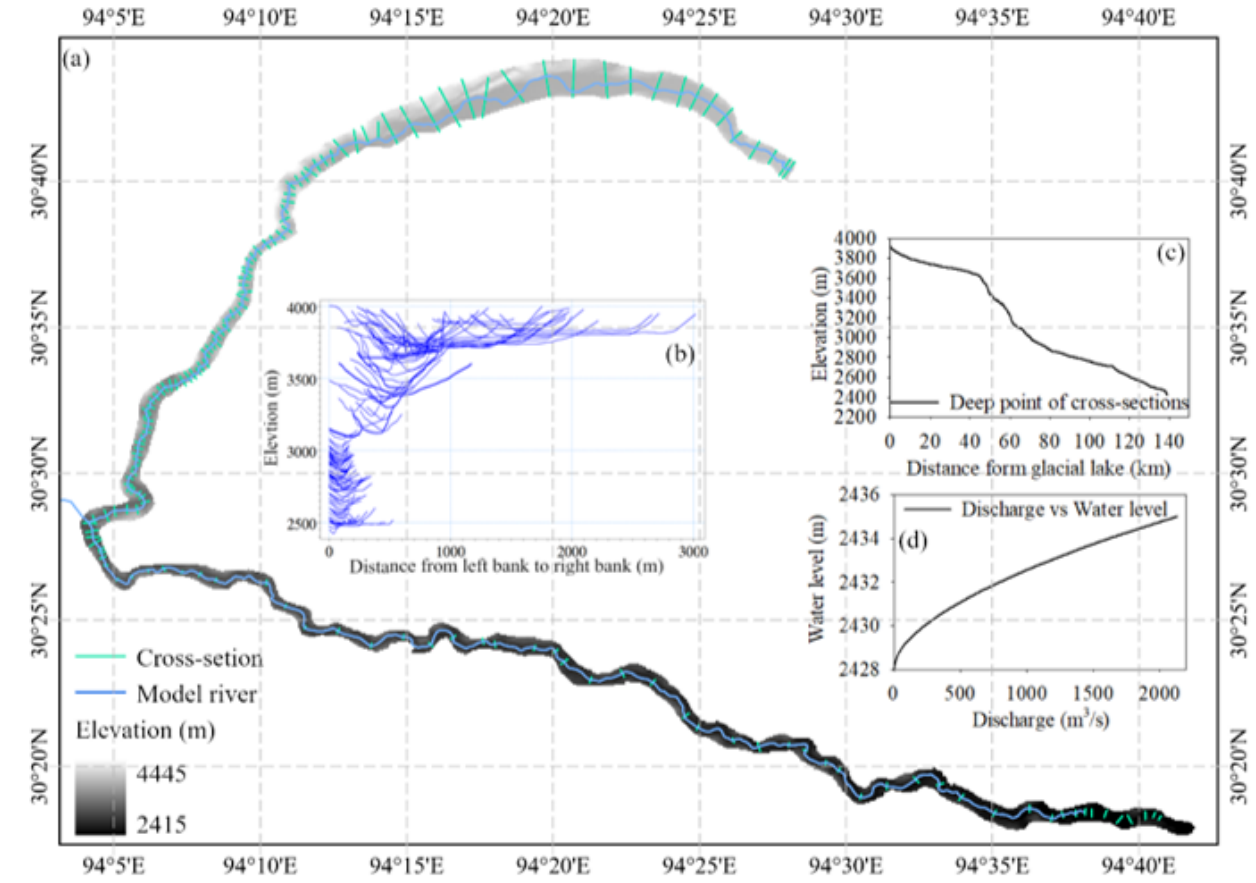

Figure 2

The river channel, cross-sections, and downstream open boundary of the study area

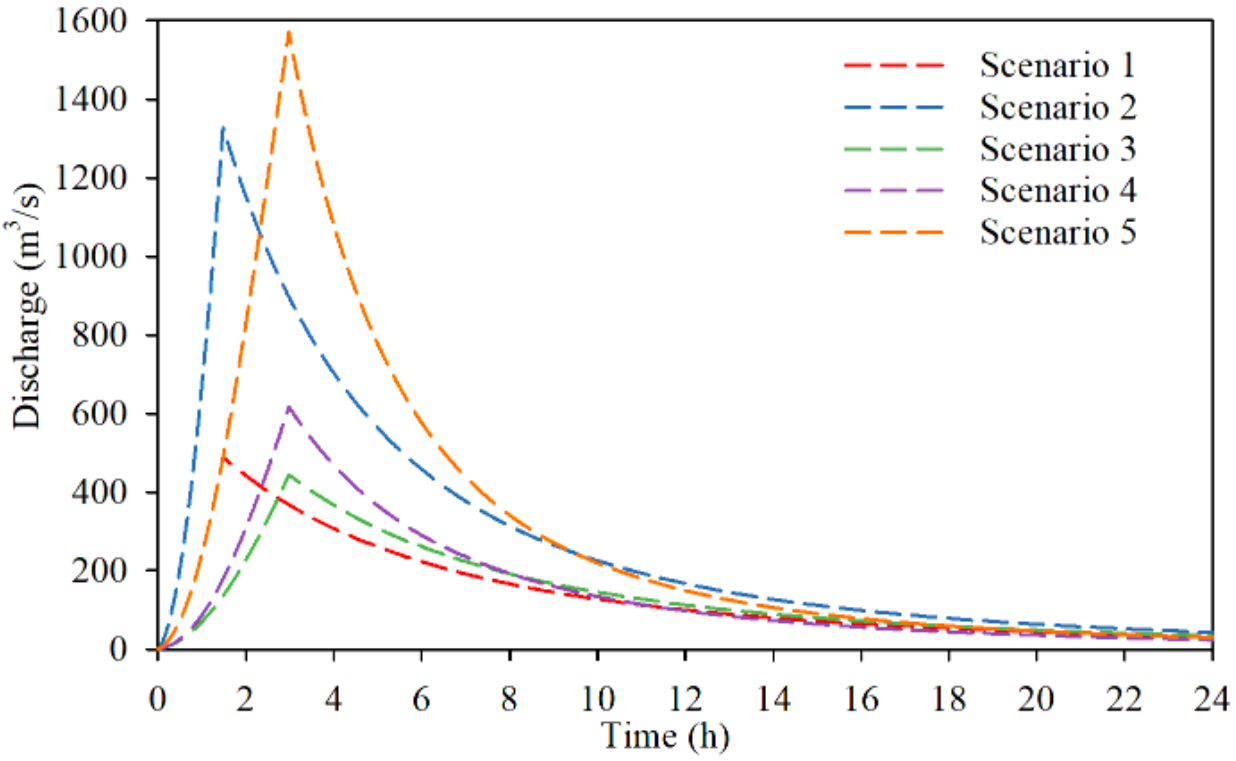

Figure 3

GLOFs hydrographs of different scenarios at breach outlet

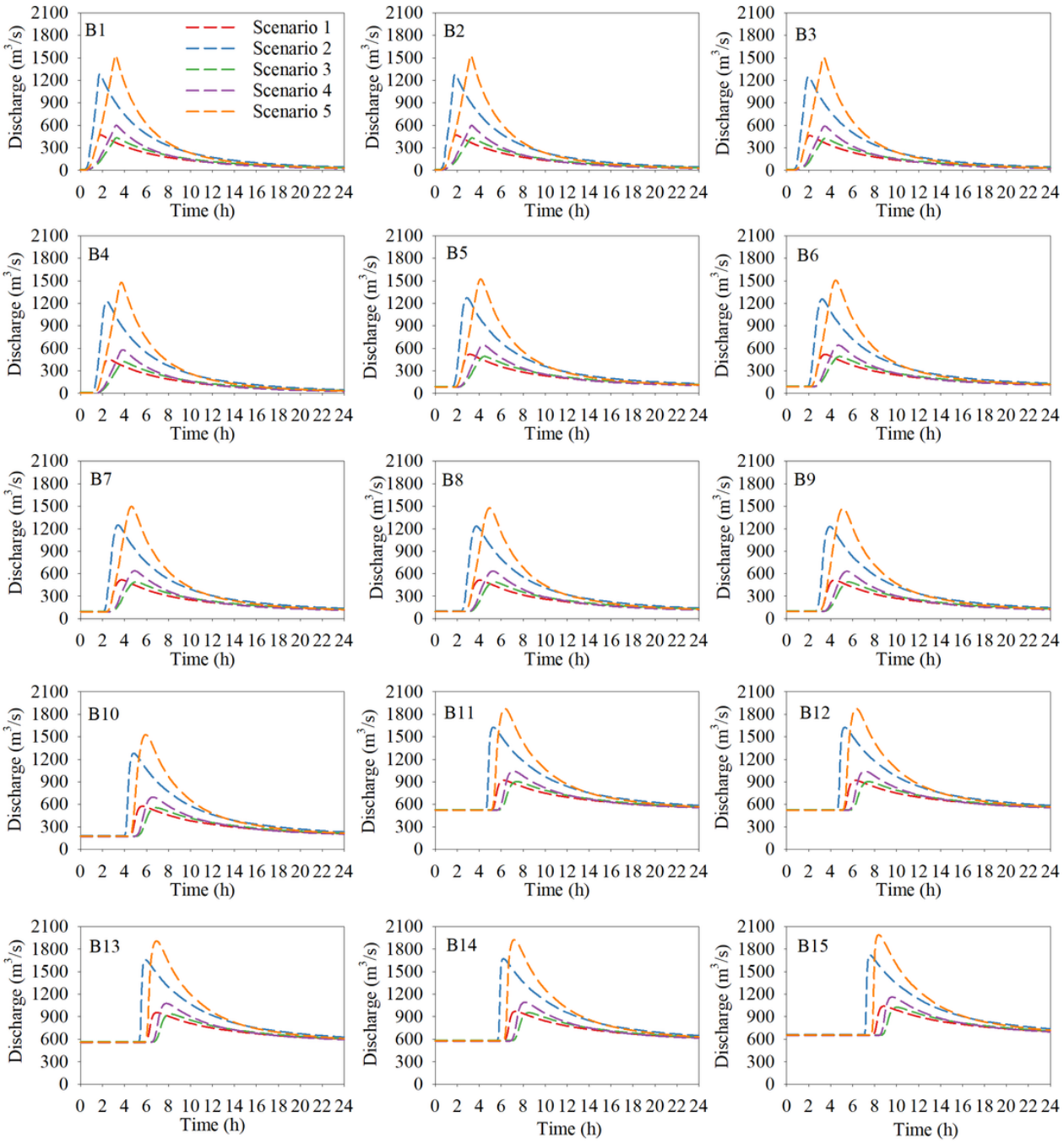

Figure 4

GLOFs hydrograph of different scenarios at 15 bridge sites

Supplementary Files

This is a list of supplementary files associated with this preprint. Click to download.

- Table5GLOFspeakdischarge.docx